Use of Finite Element Method for the Numerical Analysis of Eddy Current Brake

M. Talaat[1*] and N. H. Mostafa[2]
[1]Electrical Power and Machines Department – Faculty of Engineering – Zagazig University
[2]Mechanical Power Department – Faculty of Engineering – Zagazig University
Zagazig - Egypt
[*]m_mtalaat@eng.zu.edu.eg

***Abstract*—Eddy current brake is developed to take the superior advantages of fast anti-lock braking to the conventional hydraulic brake systems. Magnetic and electric field generated by these eddy currents suppress the disturbing field. The electric and magnetic field distribution are obtained from Neumann's and Maxwell's equations respectively. The presented model for simulating electric and magnetic field are a three dimensional field problem. Braking torque analysis is investigated by using an approximate theoretical model. A good agreement is found between the numerical and experimental. Since the eddy-current problem usually depends on the geometry of the moving conductive sheet and the pole shape, there is no general method for solving it analytically. This paper presents a method for analysis of the eddy current in the special case of a rotating disc in a time-variant field by using a time-domain Finite Element Method from t = 0 to the brake time. Finite Element Methods is adopted for this work using COMSOL Multiphysics model.**

Keywords— Eddy current simulation; Induced current density; Finite element method; Braking torque; Power dissipation; COMSOL Multiphysics model.

I. INTRODUCTION

Dampers have been thoroughly studied and have many different operating principles (Friction damper, Electrorheological and Magnetorheological dampers and Eddy current dampers) [1, 2].

A Friction Damper (FD) is composed of an actuator that applies a normal force on the output shaft. A frictional damping force is produced as a consequence of relative motion. If the friction damper is properly controlled it can emulate viscous characteristics or any other type of nonlinear damping. FD, pointed out in [3], are hysteresis and the presence of a static friction band [4] that can cause irregular behavior.

Electrorheological (ER) and Magnetorheological (MR) dampers use liquids whose viscosity depends on the electric or magnetic field strength respectively [1, 4-9]. A more accurate model and a comparison between MR and FD can be found in [3], where it is pointed out that MR damper, like the FDs, present high hysteresis.

Eddy Current Damper (ECD) is magnetic devices composed of a conductive material moving through a magnetic field. Eddy currents are induced and create a damping force that is proportional to the relative velocity between the material and the magnetic field.

These devices can be realized with either permanent magnets or electromagnets. In both cases there is the possibility to design a device whose damping can be adjusted [10-13]. In one case, the damping coefficient can be controlled by varying the intensity of the magnetic field, in the other case, by modifying the geometry of the conductor, or the gap between the conductor and the magnets [12]. This class of devices, being fluid-free and contact-free, is not affected by typical troubles due to oil, and by frictional wear. The conventional contact type brake system which uses a hydraulic system has many problems such as time delay response due to pressure build-up, brake pad wear due to contact movement, bulky size, and low braking performance in a high speed region.

The simulation of magnetic and electric field plays an important role in the understanding of eddy current phenomena, especially in the composite conducting medium. Numerical methods, such as finite element Method (FEM) [14], charge simulation method (CSM) [15-21], and integral equation methods have been used to simulate the electric and magnetic fields.

In this paper, a contactless brake system using an eddy current is proposed to overcome the problems. The analysis of the eddy current density distribution and the braking torque are presented for a rotating disc which has a finite radius. The simulation of the induced magnetic, electric fields and eddy current in conducting disc considered this model as a three-dimension field problem. Hence, accurate computations of magnetic and electric field are a prerequisite for determining the calculating induced eddy current. The Finite Element method (FEM) is used for the distribution of eddy current in the rotating conductive disc.

II. BRAKING TORQUE ANALYSIS

Figure 1, given by [17] explains how the eddy current is induced when a magnetic flux goes through a rotating disc of conductive material. Due to the interaction between the eddy current and a magnetic flux, a braking force is generated. This force, Lorentz forces, from the currents slow the disc rotation.

The eddy current had been explained by many analytical methods. One of them calculated the amount of eddy current and braking torque by assuming that all the power dissipated by the eddy current is used for generating the braking torque.

* Corresponding author (M. Talaat) Editor board member of Journal of Electrical Engineering (JEE).

The other obtained the braking force by applying the Lorentz force law while using an imaginary current path lumped on the disc and resistance obtained by experiment.

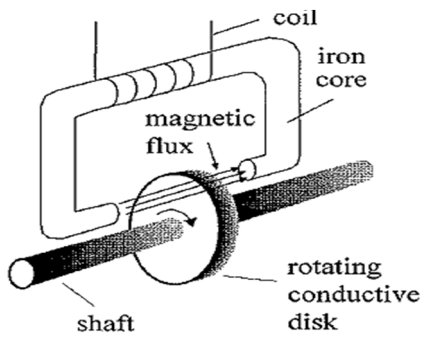

Fig. 1. A schematic configuration of an eddy current type brake system [17].

In this paper the braking system is applied by using a finite element method to the general diffusion equation derived from Maxwell's equation for the study of the transient and steady state eddy current effects.

III. Simulation Model

From Lorentz force the velocity v at a point (x, y) due to the induced current from a rotating disc with angular velocity ω about its axis, is given by

$$v = \omega(-y, x, 0) \tag{1}$$

For a conductive rod of length l moving with the constant velocity, v, perpendicular to the axial direction of the conductive rod in a time-variant magnetic field B. The motional electric field intensity E_m induced in the conductive rod can be calculated as [18-19]

$$E_m = (E + v \times B) \tag{2}$$

where, E is the electric field intensity obtained by Coulomb's law.

Since there is no complete circuit the motional electric field intensity E_m is zero. Hence, E in the conductive rod equals

$$E = -v \times B \tag{3}$$

The movable charges of the conductor are subject to the magnetic force $Qv \times B$ that is directed downward along the conductive rod. This will lead to a separation of the charges Q, the positive ones moving to one side of the conductive rod and the negative ones to the other side. But these separated charges will produce an electric field E pointing upward that will tend to decrease the total force on the given charge moving in the interior.

The magnetic current density J_m is determined from time-varying Maxwell's equation [18-19] as

$$J_m = \nabla \times H \tag{4}$$

where, H is the magnetic field strength which equal to $\mu^{-1}B$ with

$$B = \nabla \times A \tag{5}$$

$$J_m = \nabla \times (\mu^{-1} \nabla \times A) \tag{6}$$

and an electrostatic current density, at time $t = 0$, J_e is given as

$$J_e = \sigma E_e \tag{7}$$

where, σ is the conductivity of the conductor materials and the static electric field intensity E_e is given as

$$E_e = -\nabla \emptyset \tag{8}$$

where, $\emptyset$ is the scalar electric potential. Equation (7) can be modified to

$$J_e = -\sigma \nabla \emptyset \tag{9}$$

The eddy current density outside the pole projection area, J_r , is represented simply by

$$J_r = \sigma E \tag{10}$$

from eqns. (3) and (5) the motional current density is equal to

$$J_r = -\sigma v \times (\nabla \times A) \tag{11}$$

According to Kirchhoff's current law, the summation of current is equal to zero, taking into account the current direction. A new equation is produced to simulate the eddy current as

$$\nabla \times (\mu^{-1} \nabla \times A) - \sigma v \times (\nabla \times A) + \sigma \nabla \emptyset = 0.0 \tag{12}$$

A new equation is produced to simulate the eddy current using FEM the boundary condition at $t = 0$ is $(\nabla \cdot J = 0)$ with $J_m = 0$

$$-\nabla \cdot (-\sigma v \times (\nabla \times A) + \sigma \nabla \emptyset) = 0.0 \tag{13}$$

The other boundary condition depends on the magnetic and electric boundary conditions on external boundaries are

$$\left.\begin{array}{l} n \times A = 0 \\ n \cdot J = 0 \end{array}\right) \tag{14}$$

where, n is the normal component of the boundary value.

The induced vertical torque, T_z, slows the disc down, which described by an ordinary differential equation (ODE) for the angular velocity ω

$$T_z = I \frac{d\omega}{dt} \tag{15}$$

where, I is the moment of inertia given by;

$$I = m \frac{r^2}{2} \tag{16}$$

where, r is the finite radius of the disc and m is the disc mass

The total torque T is obtained by volume disc integration

$$T = \int_{\text{disc volume}} r \times (J \times B)\, dv \tag{17}$$

Owing to the symmetry of the disc, the problem space can be restricted to upper view of the disc with appropriate symmetry boundary conditions, Fig. 2 [22-23]. The upper view

of the disc is a 1 cm thick copper disc with a radius of 10 cm and an initial angular speed of 1000 rpm, with two variable magnetic flux density B = 1 T and B = 2 T, hard ($\mu_r = 1$) permanent magnet connected to an iron yoke with a 1.5 cm air gap in which the copper disc spins.

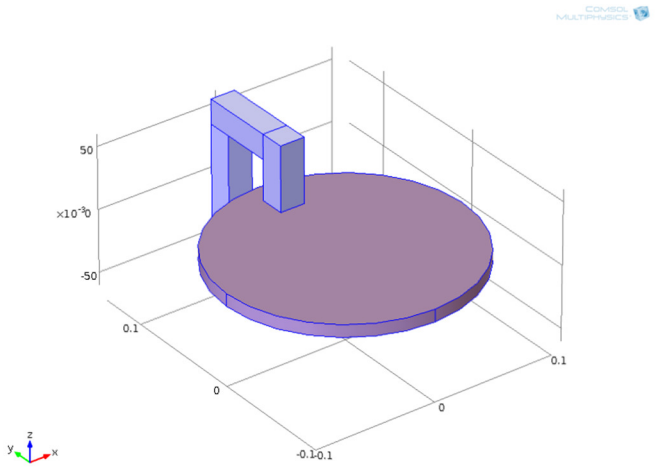

Fig. 2. Three dimension model of braking system using eddy current brake [22-23].

Numerical calculations were performed using partial differential equations (PDE) solutions [14, 20], using COMSOL Multiphysics program Model [22-23] but with more details for the three kinds of current given in Eqs (6), (9) and (11). In general, a three-dimensional (3D) problem space is divided into triangular elements and the variables are approximated by third order polynomials in each element, see Fig. 3. The boundary condition that the radial component of the eddy currents is zero at the edge of the rotating disc is assumed.

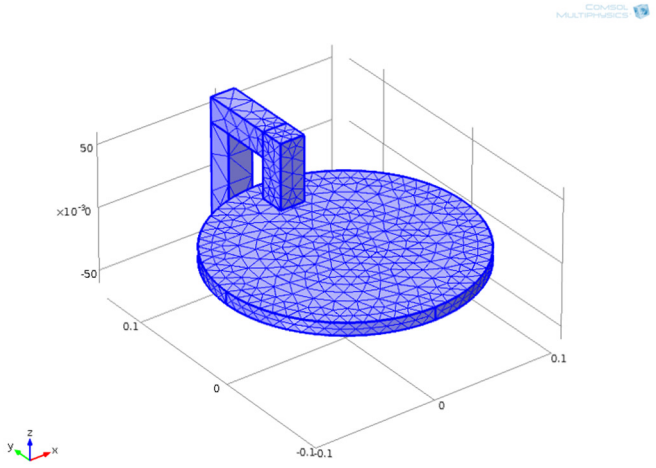

Fig. 3. Finite element discretization results 15689 nodes and 38584 elements [22-23].

IV. Results and Discussion

A. Braking Performance

In order to demonstrate the proposed approach, the COMSOL Multiphysics model is set up as shown in Fig. 3.

Figures 4, 5, and 6 show the time evolution of the angular velocity, braking torque and dissipated power respectively.

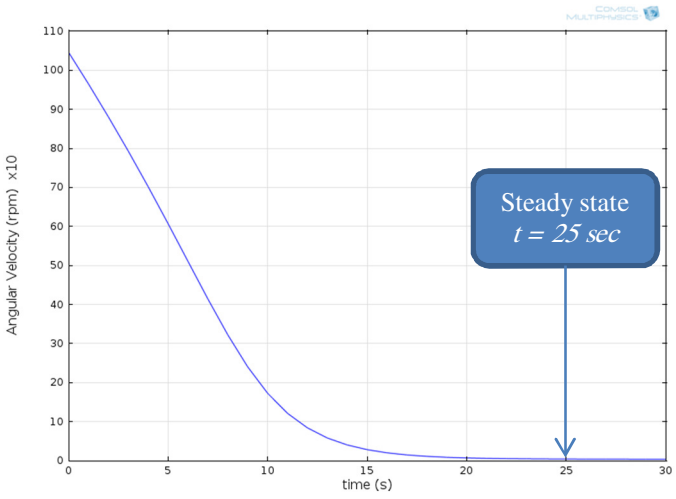

(a)

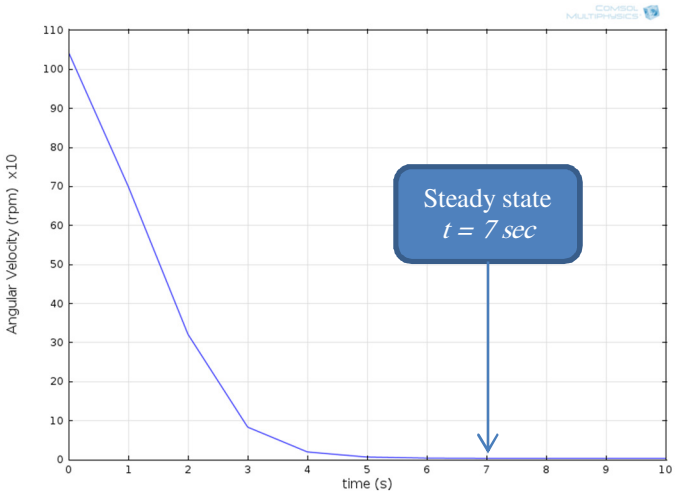

(b)

Fig. 4. The time evolution of the angular velocity with an initial angular speed of 1000 rpm, (a) for $B = 1\,T$ and (b) for $B = 2\,T$.

From Fig. 4, it is clear that the damping coefficient can be controlled by varying the intensity of the magnetic field and the magnetic flux density, in the other case, by modifying the geometry of the conductor, or the gap between the conductor and the magnets.

The disc is assumed to start moving with rolling motion which has a linear disc velocity of 10.5 m/s which corresponds to initial wheel angular velocity of 1000 rpm. From Fig. 4, the angular velocity of the moving disc has almost stopped at t = 25 s for B = 1 T and t = 7 s for B = 2 T.

From Fig. 5, the maximum value of the braking force is assumed to be 0.5 Nm, the braking torque value increases with magnetic flux value.

The Dissipation power increases as the induced eddy current density increases see Fig. 6, from this figure it is clear that the eddy current braking have the disadvantage of consuming power and produce heating while maintaining a fixed damping value.

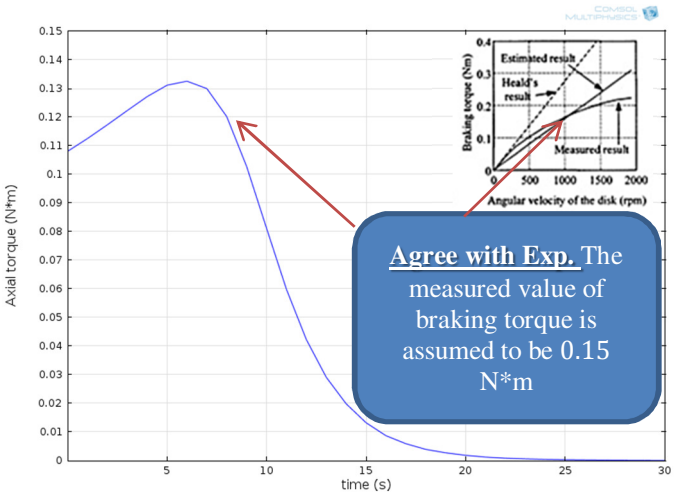

(a)

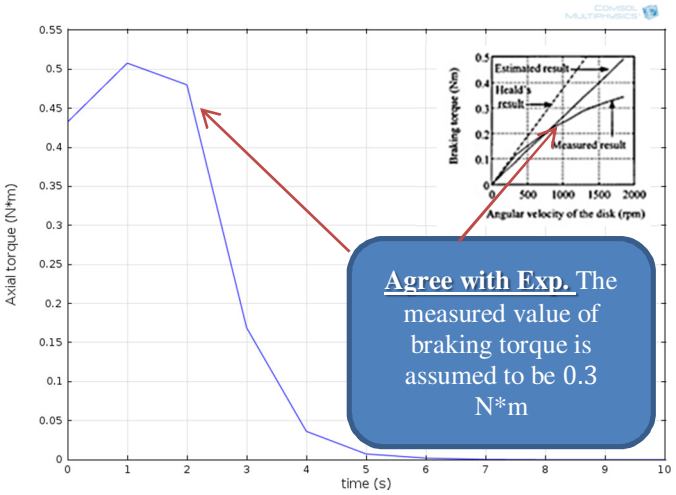

(b)

Fig. 5. The time evolution of the braking torque with an initial angular speed of 1000 rpm, (a) for $B = 1\ T$ and (b) for $B = 2\ T$.

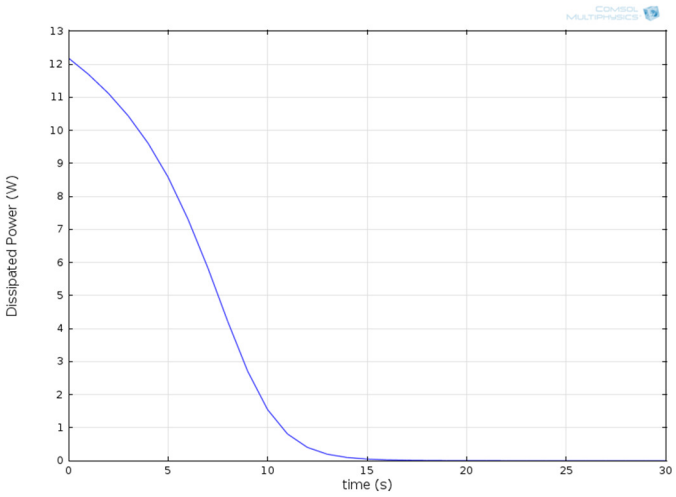

(a)

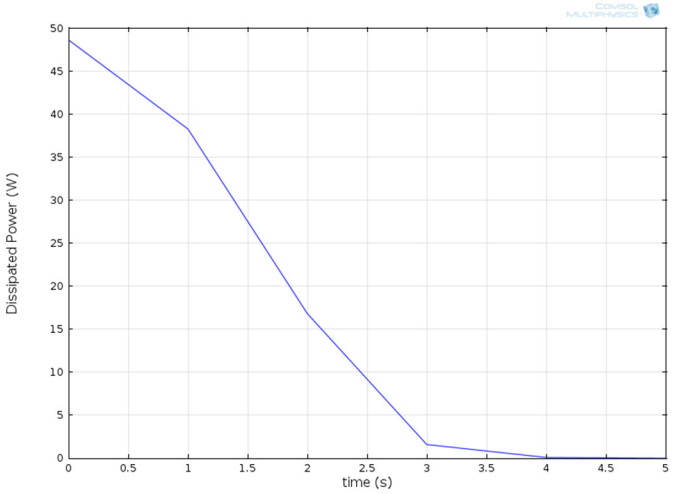

(b)

Fig. 6. The time evolution of the dissipated power with an initial angular speed of 1000 rpm, (a) for $B = 1\ T$ and (b) for $B = 2\ T$.

B. Eddy Current Density

The simulation program gives the initial value and direction of the eddy current density before rotational at time $t = 0$ s for the two cases, $B = 1$ T and $B = 2$ T respectively see Fig. 7.

The maximum value of initial current density in case of $B = 1$ T is 1.1775×10^7 A/m^2, while in case of $B = 2$ T is 2.353×10^7 A/m^2.

From Figures 8 and 9, the final steady state value and direction of the eddy current density are reduced to 8.0954×10^4 A/m^2 in case of $B = 1$ T and $t = 25$ s and to 1.4356×10^5 A/m^2 in case of $B = 2$ T and $t = 7$ s. The reduction in the eddy current density value can be attributed to the induced magnetic flux which causes the reduction of the net magnetic flux passing through the pole projection area and the temperature dependency of the conductivity.

According to the boundary condition it is cleared that the radial component of the eddy currents is zero at the edge of the rotating disc, shown in Figures 8, and 9.

I. Experimental Model

To validate the accuracy of the proposed model, the braking torque is compared with measured values by experiment. The experimental setup composed of the rotating disc and electric motor is shown in Fig. 10 [17], the physical parameters of the experimental model are as follow: the width and the height of the pole are 20 mm, air gap length 5 mm, finally the radius and thickness of the disk are 10 cm and 3 mm respectively.

Fig. 10 shows an overall experimental setup for investigating the performance of the ECB.

Fig. 11 shows experimental and simulation results of how the brake system performs for the scaled model. For a comparison purpose, the simulation results are displayed together with the experimental results.

The disc is assumed to start moving with rolling motion which has a linear angular velocity of 10.5 m/s which corresponds to initial wheel angular velocity of 1000 rpm and copper disc radius of 10 cm. Hence, the experimental model

with respect to angular velocity and copper disc radius agree well to the simulation model.

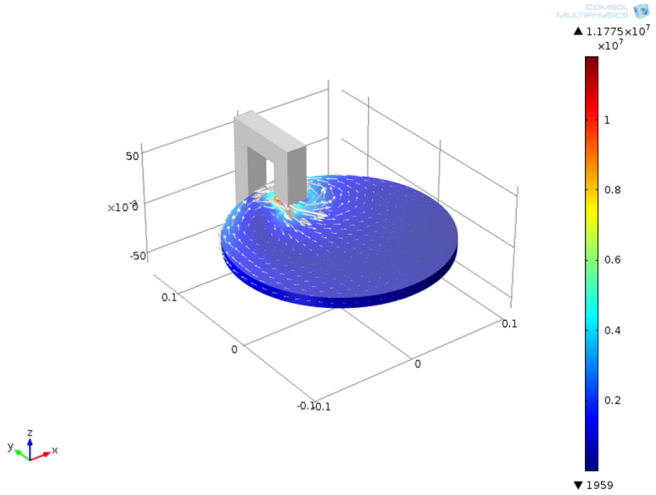

(a)

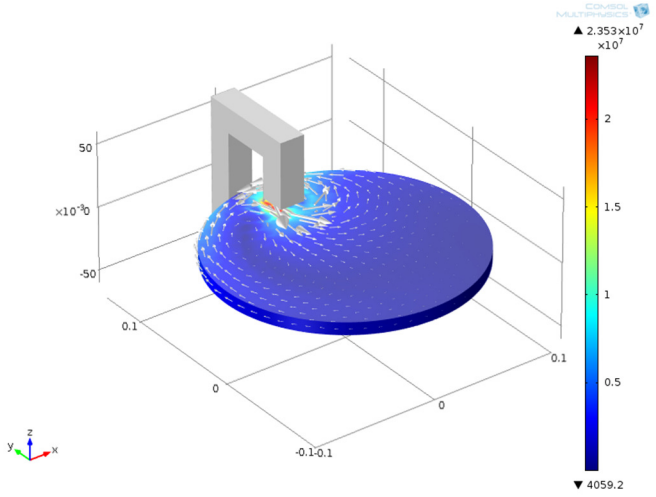

(b)

Fig. 7. The eddy current density magnitude and direction at $t = 0\ s$ with an initial angular speed of 1000 rpm, (a) for $B = 1\ T$ and (b) for $B = 2\ T$.

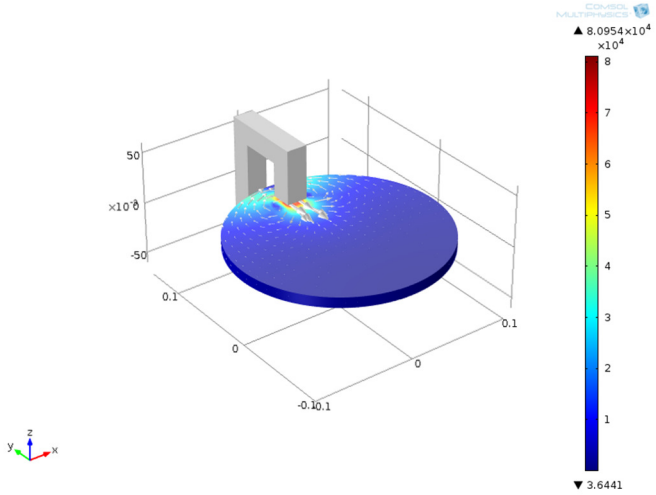

Fig. 8. The eddy current density when the disc has almost stopped $t = 25\ s$ with an initial angular speed of 1000 rpm and for $= 1\ T$.

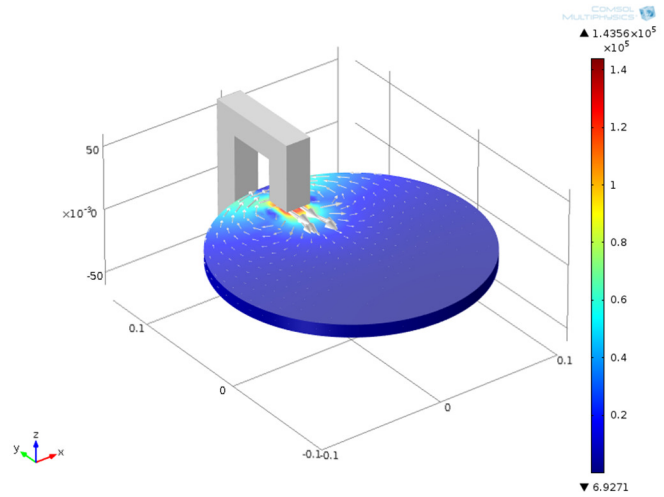

Fig. 9. The eddy current density when the disc has almost stopped $t = 7\ s$ with an initial angular speed of 1000 rpm and for $B = 2\ T$.

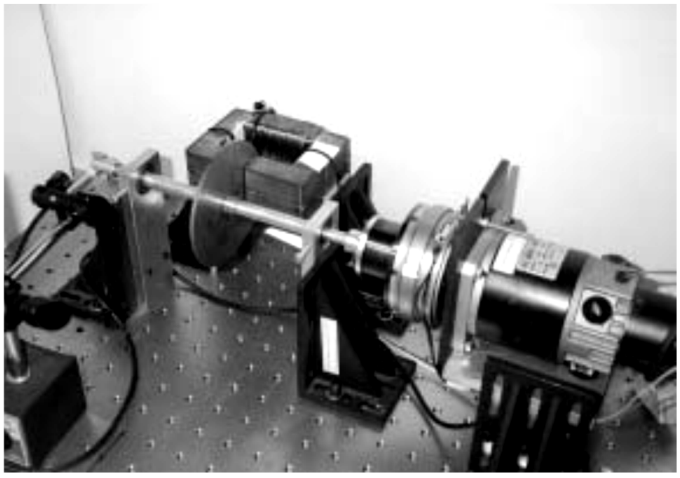

Fig. 10. An overall experimental setup for investigating the performance of the eddy current damper [17].

Fig. 11 shows experimental results for the linear velocity of the disc 10.5 m/s. In Fig. 11(b), the maximum value of the estimated and measured results of braking torque is assumed to be 0.15 when angular velocity 1000 rpm, which agree with Fig. 5(a) and in Fig. 11(c), the maximum value of the estimated and measured results of braking torque is assumed to be 0.3, which agree with Fig. 5(b). These results obtained from the assumed simulation model.

II. Conclusion

The analyses of the eddy current density distribution and the braking torque are presented for the rotating disc. An approximate theoretical model is derived for the behavior of an eddy current disc brake in the low-speed zone. For this purpose, the eddy current density in the rotating disc was obtained by using FEM due to the motional induced electric field. The boundary condition that the radial component of the eddy currents is zero at the edge of the rotating disc is assumed. To validate the proposed model, the braking torque of the analytical result is compared with the others experimental result. The proposed model presents fairly accurate results in a low angular velocity range. Braking torque analysis is

performed by using an approximate theoretical model and the braking torque is experimentally compensated. From simulation and experimental results, it is observed that the eddy current brake provides a fast braking response because it is capable of fast anti-lock braking. In order to make the proposed method helpful in practical problems, the induced magnetic field of the conductivity taking into considered. In conclusion, it can be said that an ECB can provide superior performances in terms of reliability and safety in a high speed region when it is compared with the performance results of the conventional hydraulic brake.

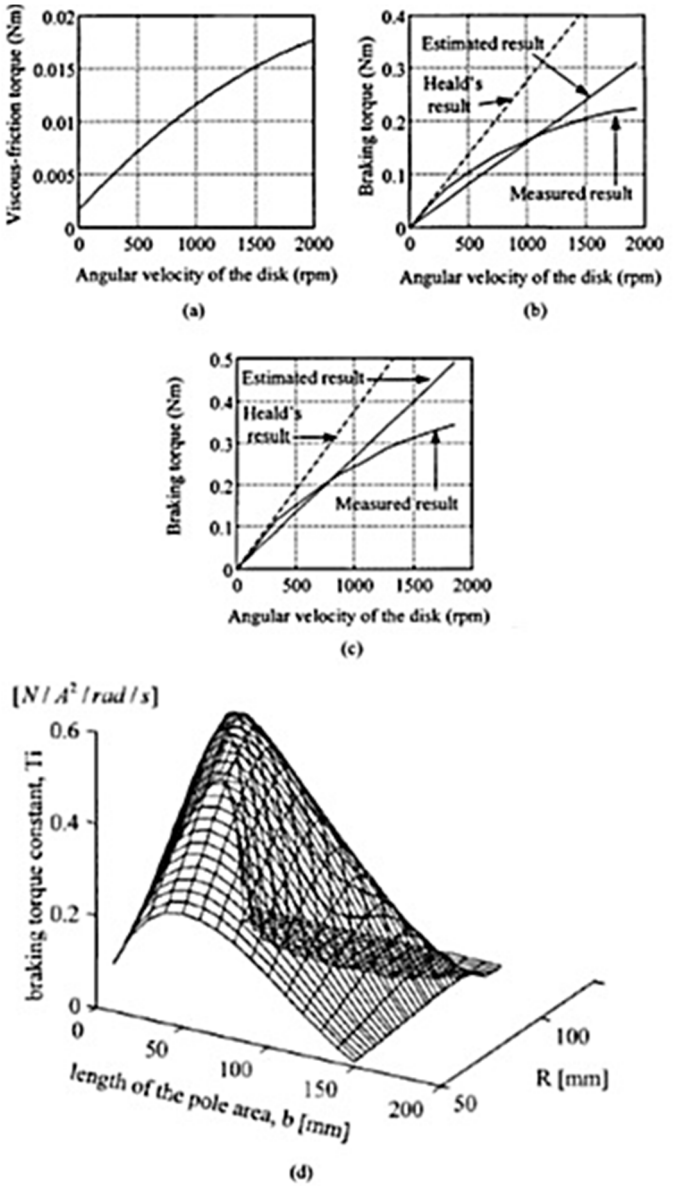

Fig. 11. Experimental results of (a) the viscous-friction torque, (b) the braking torque when $B = 1\,T$, (c) the braking torque when $B = 2\,T$, (d) Simulation results of the braking performance of the ECB when angular velocity is ω is 1000 rpm and copper disc radius of 10 cm [17-18].

REFERENCES

[1] C. Chew, G. Hong, W. Zhou, Series damper actuator: a novel force/torque control actuator, in: 4th IEEE/RAS International Conference on Humanoid Robots, Vol. 2, 2004, pp. 533–546.

[2] H. Iwata, S. Sugano, Design of human symbiotic robot TWENDY-ONE, in: IEEE International Conference on Robotics and Automation, ICRA 2009, 2009, pp. 580–586

[3] E. Guglielmino, C. Stammers, K. Edge, Damp-by-wire: magnetorheological vs friction dampers, in: 16th IFAC World.

[4] J. C. Dixon, "The Shock Absorber Handbook, in: Senior Lecture in Engineering Mechanics", PEP, Wiley, 2007.

[5] E. Garcia, J. Arevalo, F. Sanchez, J. Sarria, P. Gonzalez-de Santos, Design and development of a biomimetic leg using hybrid actuators, in: IEEE/RSJ International Conference on Intelligent Robots and Systems, IROS 2011, 2011, pp. 1507–1512

[6] D. Chapuis, R. Gassert, E. Burdet, H. Bleuler, A hybrid ultrasonic motor and electrorheological fluid clutch actuator for force-feedback in MRI/fMRI, in: 30th Annual International Conference of the IEEE Engineering in Medicine and Biology Society, EMBS 2008, IEEE, 2008, pp. 3438–3442.

[7] P. Fauteux, M. Lauria, B. Heintz, F. Michaud, Dual-differential rheological actuator for high-performance physical robotic interaction, IEEE Transactions on Robotics 26 (4) (2010) 607–618.

[8] J. Li, D. Jin, X. Zhang, J. Zhang, W. Gruver, An electrorheological fluid damper for robots, in: IEEE International Conference on Robotics and Automation, ICRA 1995, 1995, pp. 2631–2636.

[9] J. Desrosiers, J.L. Bigué, M. Denninger, G. Julió, J. Plante, F. Charron, Preliminary investigation of magneto-rheological fluid durability in continuous slippage clutch, Journal of Physics: Conference Series 412 (2013) 012022.

[10] B. Ebrahimi, M.B. Khamesee, F. Golnaraghi, A novel eddy current damper: theory and experiment, Journal of Physics D: Applied Physics 42 (7) (2009) 075001.

[11] A. H. C. Gosline, V. Hayward, Eddy current brakes for haptic interfaces: design, identification, and control, IEEE/ASME Transactions on Mechatronics 13 (6) (2008) 669–677.

[12] H. A. Sodano, J.-S. Bae, D. Inman, K. Belvin, Improved concept and model of eddy current damper, Transaction of the ASME 128 (2006) 294–302.

[13] A. Mohand-Ousaid, G. Millet, S. Régnier, S. Haliyo, V. Hayward, Haptic interface transparency achieved through viscous coupling, The International Journal of Robotics Research 31 (3) (2012) 319–329.

[14] M. Talaat, A. El-Zein, "A numerical model of streamlines in coplanar electrodes induced by non-uniform electric field", Journal of Electrostatics Vol. 71, No. 3, pp. 312-318, 2013.

[15] A. El-Zein, M. Talaat and M. M. El Bahy, "A Numerical Model of Electrical Tree Growth in Solid Insulation" IEEE Trans. on Diele. Elec. Ins., Vol. 16, No. 6, 2009, pp. 1724-1734.

[16] M. Talaat, "Calculation of Electrostatically Induced Field in Humans Subjected to High Voltage Transmission Lines", Electrical Power System Research Vol. 108, pp. 124-133, 2014.

[17] Kapjin Lee and Kyihwan Park, "Optimal robust control of a contactless brake system using an eddy current", Mechatronics, Vol. 9, pp. 615-631, 1999.

[18] Kapjin Lee and Kyihwan Park, "Modeling Eddy Currents With Boundary Conditions by Using Coulomb's Law and the Method of Images", IEEE Trans. on Magnetics, Vol. 38, No. 2, 2002, pp. 1333-1340.

[19] M. Talaat, "Calculation of Electric and Magnetic Induced Fields in Humans Subjected to Electric Power Lines", Journal of Electrostatics Vol. 72, No. 5, pp. 387-395, 2014.

[20] M. Talaat, "Influence of Transverse Electric Fields on Electrical Tree Initiation in Solid Insulation", IEEE Annual Report Conference on Electrical Insulation and Dielectric Phenomena CEIDP 2010, pp. 313-316, USA, October 17-20, 2010.

[21] M. Talaat, "Electrostatic Field Calculation in Air Gaps with a Transverse Layer of Dielectric Barrier", Journal of Electrostatics Vol. 72, No. 5 pp. 422-427, 2014.

[22] http://www.comsol.com/model/simulation-of-a-magnetic-brake-2014

[23] http://www.comsol.com/blogs/simulating-eddy-current-brakes/